C. H. M. Broeders and A. Yu. Konobeyev

Production of ^{4}He and ^{3}He from tantalum and tungsten irradiated with nucleons at energies up to 1 GeV

The comparison of different methods of calculation and computer codes used to obtain helium isotope production cross-sections for nuclear reactions induced by nucleons at energies up to 1 GeV was performed. The cross-sections were calculated using the GNASH code, the modified ALICE code, the DISCA code and the CASCADE/INPE code. The evaluation of the helium production cross-section for tantalum and tungsten was performed using the results of model calculations, available experimental data and systematics predictions. The cross-sections were obtained for nuclear reactions induced by neutrons and protons at energies up to 1 GeV.

Erzeugung von ^{4}He und ^{3}He aus Tantal und Wolfram bestrahlt mit Nukleonen bei Energien bis zu 1 GeV. *Ein Vergleich von verschiedenen Berechnungsmethoden und Computercodes wurde durchgeführt, die verwendet werden um Wirkungsquerschnitte für die Erzeugung von Heliumisotopen aus Kernreaktionen von Nukleonen bei Energien bis zu 1 GeV zu erhalten. Die Wirkungsquerschnitte wurden berechnet mit Hilfe des Rechencodes GNASH, dem modifizierten ALICE Code, dem DISCA Code und dem CASCADE/INPE Code. Die Heliumerzeugungsquerschnitte für Tantal und Wolfram wurden ausgewertet mit Hilfe von Modellrechnungen, verfügbaren experimentellen Daten und systematischen Vorhersagen. Die Wirkungsquerschnitte wurden bestimmt für Kernreaktionen induziert durch Neutronen und Protonen bei Energien bis zu 1 GeV.*

1 Introduction

The study of helium production in nuclear reactions induced by intermediate and high energy protons is an important part of the investigation of radiation durability of materials designed for accelerator driven systems (ADS), neutron generators and other emerging nuclear energy systems. Helium generation and accumulation in materials results in significant change in physical properties of irradiated materials.

Recently the determination of reliable helium production cross-sections for tantalum and tungsten has got a special interest for the TRADE project [1]. Tantalum and tungsten are proposed as materials of the solid target, which subjected to the primary proton beam irradiation as the irradiation by secondary neutrons produced in the target.

The goal of this work is the evaluation of the helium production cross-section for tantalum and tungsten irradiated with neutrons and protons at energies from several MeV up to 1 GeV. This energy range covers most of possible proton irradiation conditions in the ADS systems and neutron generators. The evaluation includes the analysis of available experimental data and the contents of evaluated data libraries, the calculations by theoretical models and systematics.

The brief description of the models used for the cross-section calculation is given in Section 2. Section 3 presents the comparison of the results of calculations with experimental data. The evaluation of the helium production cross-section is discussed in Section 4.

2 Brief description of models and codes for ^{4}He and ^{3}He production cross-section calculation

The Section describes briefly nuclear models, approaches and codes used in the present work for the calculation of the yield of helium isotopes in nuclear reactions induced by nucleons.

2.1 Pre-compound and evaporation models

2.1.1 The GNASH code

The code [2] implements the pre-equilibrium exciton model in a "closed" form and the equilibrium model considering effects of angular momentum and parity conservation. The exciton level density is calculated according to Williams [3]. The averaged squared matrix element for two-body interaction is obtained from the parameterization [4] by the set of functions of E/n, where E is the excitation energy and "n" is the number of excitons. The density of states available for transitions from "n" to "n + 2" and "n – 2" exciton states is calculated according to Refs. [2, 5].

The multiple pre-equilibrium nucleon emission is described according to Refs. [6, 7]. The consideration is limited by two pre-compound nucleons escape.

The pre-equilibrium α-particle emission spectrum for nucleon induced reaction is calculated as a sum of components corresponding to the mechanism of pick-up and knock-out. The components are evaluated according to the phenomenological Kalbach approach [5]. The pre-equilibrium emission of α-particles following the nucleon emission, i. e. the multiple pre-compound α-emission is not considered.

Equilibrium particle emission is described with the help of the Hauser-Feshbach model [2]. The model is combined with the pre-equilibrium exciton model as discussed in Refs. [2, 9]. In the present work two different approaches are used for the nuclear level density calculation in equilibrium states: the

Fermi gas model with the nuclear level density parameter depending from the excitation energy [10] and the generalized superfluid model [11].

The optical potentials from Refs. [12, 13] are used for the calculation of the reaction cross-section and transmission coefficients.

2.1.2 The ALICE/ASH code

The code implements the geometry dependent hybrid model [14] and the evaporation Weisskopf-Ewing model [15]. The ALICE/ASH code is an advanced version of the original Blann code [16]. Modifications concerns the implementation in the code the models describing the pre-compound composite particle emission [17–19] and the fast γ-emission [20], various approaches for the nuclear level density calculation [21–23] and the model for the fission fragment yield calculation [24].

The multiple pre-compound emission is described by the approximate approach [14]. As in the GNASH code, only two fast nucleon escapes are considered. The pre-equilibrium α-particle emission spectrum is calculated as a sum of components corresponding to the mechanism of pick-up, nucleon coalescence and knock-out. For ^{3}He emission the coalescence and pick-up processes are considered. The contributions of the pick-up and coalescence mechanisms are calculated with the help of the model [25, 26] combined with the hybrid exciton model, as described in Ref. [17]. The absorption rate for complex particles is defined using the imaginary part of the optical potentials.

The multiple pre-compound effects are taken into account for the α-particle emission [18]. The successive emission of three and more pre-equilibrium particles is not considered.

The same models, as in the GNASH calculations are applied to the nuclear level density calculation for equilibrium state: the Fermi gas model [10] and the superfluid model with parameters from Ref. [27].

2.2 Intranuclear cascade evaporation models

2.2.1 The DISCA-C code

The DISCA-C code [28] implements the intranuclear cascade evaporation model describing the interaction of particles with pre-formed clusters and their emission from nucleus.

In the model the nucleus is broken up into several concentric zones with uniform density approximating the Woods-Saxon distribution. It is supposed that besides of nucleons the nucleus consists of pre-formed triton, ^{3}He and α-particle clusters. The simulation of the knock-out and pick-up processes is performed as described in Ref. [28]. The reflection and refraction of particle momenta on nuclear zone boundaries is considered. The Pauli principle is taken into account as for nucleon-nucleon, as for nucleon-cluster collisions. In an addition, the restriction on the orbital momenta of nucleons and clusters after the intranuclear interactions [29, 30] is considered.

The equilibrium particle emission is described by the Weisskopf-Ewing model [15]. The nuclear level density is calculated according to the Fermi gas model at the high excitation energy and by the "constant temperature" model at low energy of excitation. The value of the nuclear level density parameter is taken equal to A/9. The inverse reaction cross-sections are calculated according to the phenomenological formulas from Ref. [31] approximating the results of optical model calculations. Evaporation is considered for neutrons, protons, deuterons, tritons, ^{3}He nuclei and α-particles.

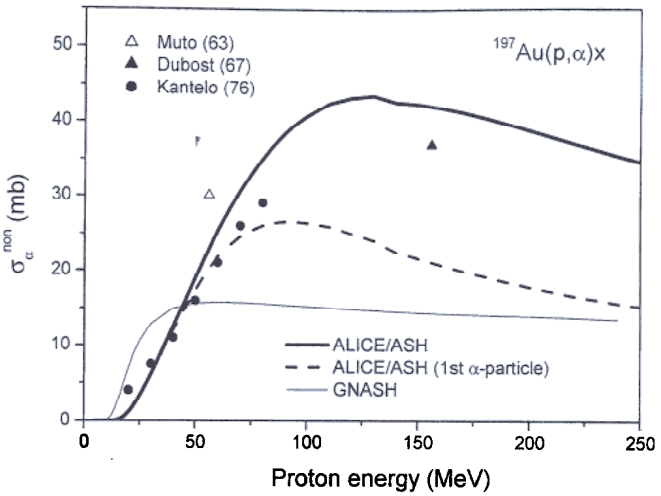

Fig. 1. The non-equilibrium component of the α-particle production cross-section for p + ^{197}Au reaction calculated by the GNASH code and the ALICE/ASH code. The measured data are from Refs. [43, 44, 46].

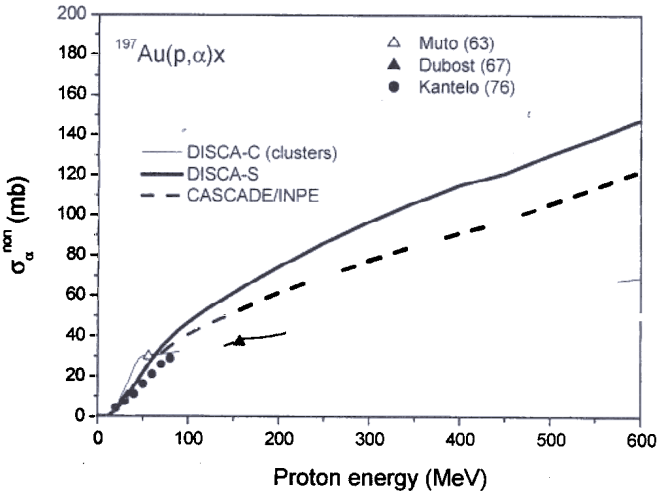

Fig. 2. The non-equilibrium component of the α-particle production cross-section for p + ^{197}Au reaction calculated with the help of the DISCA-C, DISCS-S and CASCADE/INPE codes. The measured data are from Refs. [43, 44, 46].

2.2.2 The DISCA-S code

The DISCA-S code is the simplified version of the DISCA code. The simulation of processes involving α-clusters is not performed. The model algorithm is discussed in Ref. [32, 29].

The yield of composite particles emitted during the cascade stage of nuclear reaction is described by the "nuclear bond breakdown" approach [33]. The fragment "x" formation cross-section is calculated as follows

$$\sigma_x^{casc}(E_p) = \sigma_{non}(E_p)\, N_0 (A/A_x) \left[N_{casc}(E_p)/A\right]^{m_0 \varepsilon} \qquad (1)$$

where σ_{non}(E$_p$) is the nonelastic cross-section for the interaction of the nucleus and the incident particle with the kinetic energy E_p; A_x is mass number of the fragment; A is the mass number of target nucleus; N_{casc} is the average number of nucleons emitted from nucleus on the cascade stage of the reaction; $\varepsilon = Q_x + V_x$, where Q_x is the separation energy for the fragment in the nucleus; V_x is the Coulomb potential for the fragment; N_0 and m_0 are parameters. The N_0 and m_0 values obtained in Ref. [34] are used in the present work. The Coulomb potential for α-particles is calculated as $0.21 \cdot Z + 2.5$ MeV, and for ^{3}He, as $0.21 \cdot Z$, where Z is atomic number of the target nucleus.

The nuclear density distribution is calculated as in the DISCA-C code. The Pauli principle and the restriction on the orbital momenta are checked for each intranuclear interaction. The refraction and reflection of nucleon momentum are considered at the nuclear zone boundaries. The nuclear level density for equilibrium states is calculated with the approximate formula $\rho(U) = C\exp(2\sqrt{aU})$, where a = A/9. The inverse reaction cross-section for neutrons is calculated according to Ref. [35]. The "sharp cut-off" formulas from Ref. [16] are used for the calculation of the inverse reaction cross-sections for charge particles.

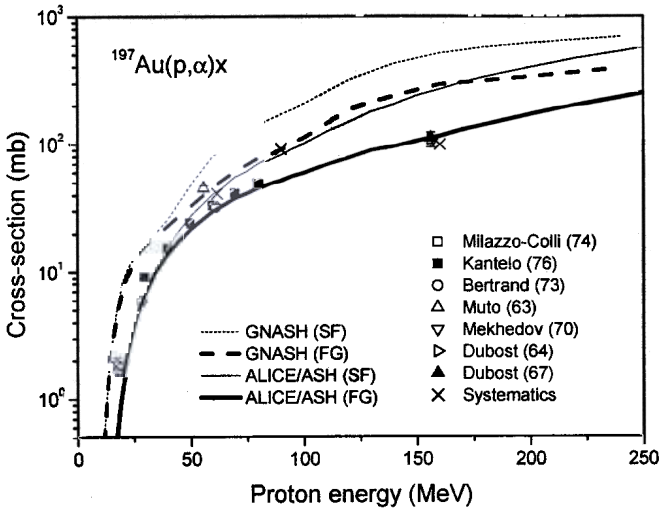

Fig. 3. The α-particle production cross-section for ^{197}Au(p, α)x reaction at the incident proton energies up to 250 MeV calculated by the GNASH code and the ALICE/ASH code using different models to obtain the nuclear level density: the Fermi gas model [10] (FG) and the superfluid model [11, 27] (SF); the cross-section estimated by systematics and data measured in Refs. [42–44, 46–49].

2.2.3 The CASCADE/INPE code

The detail description of the nuclear model implemented in the CASCADE/INPE code is given in Ref. [36, 37]. The specific features of the model include the approximation of the nuclear density by the continuous Woods-Saxon distribution, the use of the "time-like" Monte Carlo technique and the consideration of the effect of nuclear density depletion due to the fast nucleon emission.

The pre-equilibrium stage of the reaction describing by the exciton model is not considered in the present calculations, as in the DISCA-C and DISCA-S codes. After the finish of the fast particle emission the evaporation stage occurs.

The contribution of the non-equilibrium emission in the α-particle and ^{3}He-production cross-section is calculated using the approximate approach close to the model of "nuclear bond breakdown" [33]. Considering the ^{3}He and α-clusters as a stable nucleon association located on a periphery of the nucleus [32] it is easy to show, that at high projectile energies the number of clusters knocked-out from the nucleus is proportional to the number of nucleons emitted on the cascade stage of the reaction and the square of the nucleus radius. This implies, that the non-equilibrium

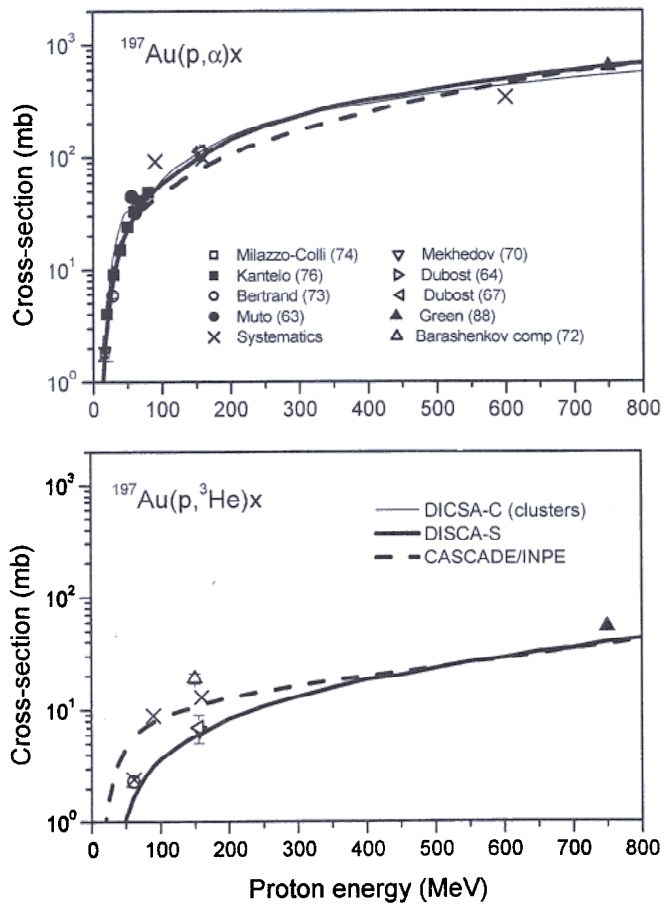

Fig. 4. The α-particle and ^{3}He production cross-section for the p + ^{197}Au reaction calculated using the DISCA-C, DISCA-S and CASCADE/INPE codes; the cross-sections estimated by systematics and measured in Refs. [42–44, 46–50].

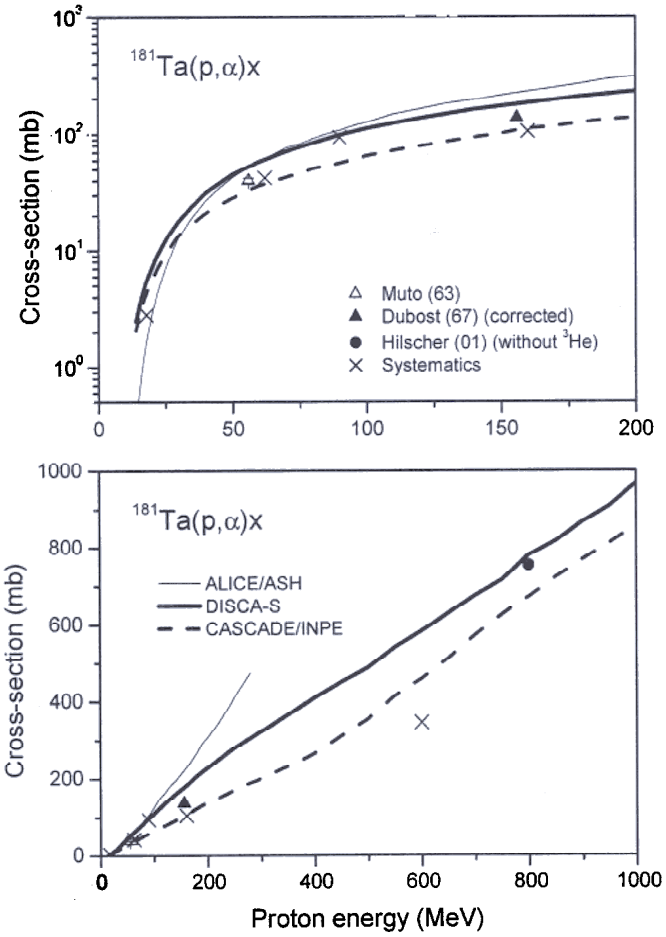

Fig. 5. The α-particle production cross-section for proton irradiation of ^{181}Ta calculated by the ALICE/ASH code, the DISCA-S code and the CASCADE/INPE code; the cross-sections estimated by systematics, measured in Ref. [44] and extracted from experimental data [43, 51].

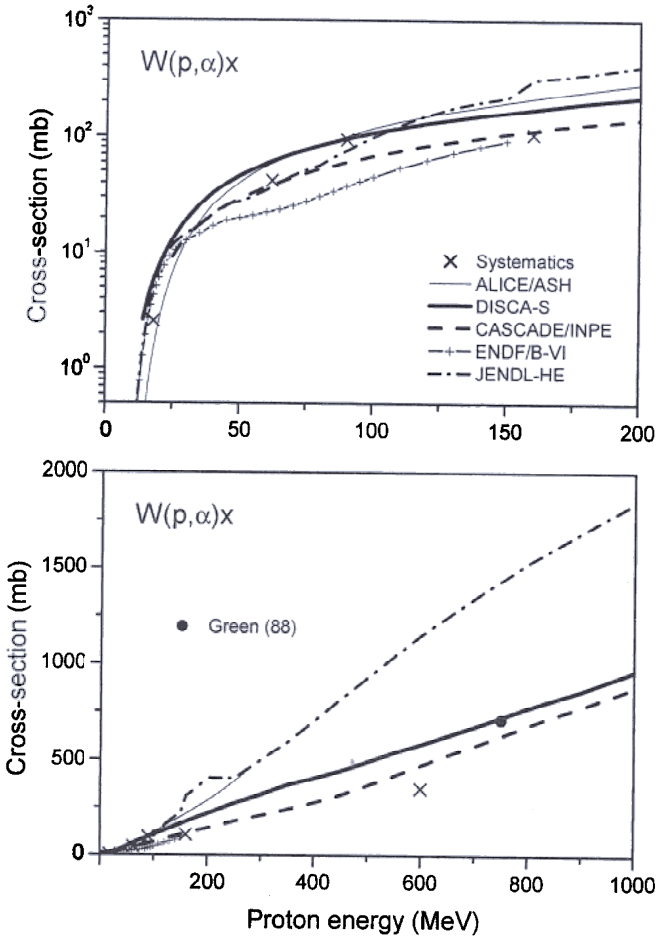

Fig. 6. The α-particle production cross-section for proton irradiation of natural tungsten calculated by the ALICE/ASH code, the DISCA-S code and the CASCADE/INPE code; the cross-sections estimated by systematics, measured in Ref. [50] and taken from ENDF/B-VI and JENDL-HE.

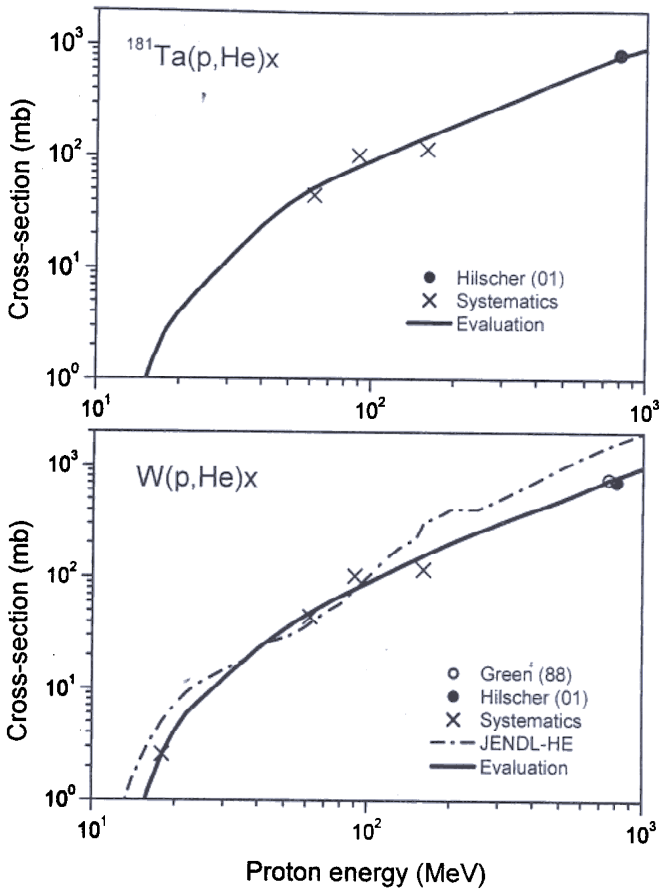

Fig. 7. The helium production cross-section ($\sigma_\alpha + \sigma_{^3He}$) for proton irradiation of ^{181}Ta and natural tungsten evaluated in the present work, estimated by systematics, measured in Refs. [50, 51] and taken from JENDL-HE.

component of the α-particle and ^{3}He production cross-section at the high energies of projectiles can be evaluated as follows

$$\sigma_x^{non}(E) = \sigma_{non}(E)\,\gamma_x N_{casc}(E) \qquad (2)$$

where γ_x is the energy independent parameter, which value should be defined from the analysis of experimental data or from independent theoretical calculations, "x" refers to the type of the cluster knocked out.

In the present work the number of cascade nucleons N_{casc} is calculated by the CASCADE/INPE code. The γ_x value is defined using the result of the ALICE/ASH code calculation at the primary proton energy around 100 MeV.

2.3 Systematics of ^{4}He and ^{3}He production cross-sections

In addition to model calculations, the ^{4}He and ^{3}He production cross-sections have been evaluated using empirical and semi-empirical formulas obtained for proton induced reactions in Ref. [38] and for neutron induced reactions in Refs. [39, 40].

2.4 Nonelastic interaction cross-sections

To exclude the discrepancy in the calculated ^{4}He and ^{3}He production cross-sections caused by the use of different reaction cross-sections (σ_{non}) the calculations by the GNASH, ALICE/ASH, DISCA-C, DISCA-S and CASCADE/INPE codes were performed with the same nonelastic reaction cross-sections. The adopted σ_{non} values were taken from ENDF/B-VI, calculated with the help of the optical model [12] or obtained from the global parameterization [41].

3 Comparison of calculations with experimental data

The available experimental data for helium isotope production in tantalum and tungsten irradiated with nucleons are not enough for detail testing of methods of the calculation. A considerable amount of experimental data for the yield of helium isotopes is available for ^{197}Au. These data are used in the present work for testing of model calculations.

Helium isotope production cross-section can be presented as a sum of the contribution of the non-equilibrium and equilibrium particle emission. The contribution of the non-equilibrium emission in the total α-particle yield has been obtained from the analyses of experimental data for ^{197}Au(p, α) x reaction in Refs. [42–46].

Fig. 1 shows the non-equilibrium component of the α-particle production cross-section (σ_α^{non}) calculated with the help of the GNASH code and the ALICE/ASH code. The contribution of the first pre-compound α-particle obtained by ALICE/ASH is also shown. The reasonable agreement is observed between the data and the ALICE/ASH calculations. The calculated σ_α^{non} cross-section passes through a maximum at 130 MeV and decreases with the primary proton energy growing. Probably, the decrease of the σ_α^{non} value is because

Table 1. The evaluated helium production cross-section ($\sigma_\alpha + \sigma_{^3He}$) for ^{181}Ta and natural tungsten irradiated with protons at energies up to 1 GeV. The cross-sections between the energy points shown should be found by the linear(x)-log(y) interpolation at energies below 14 MeV, and by the linear-linear interpolation at energies above 14 MeV

Proton energy (MeV)	Helium production cross-section (mb)	
	^{181}Ta	^{nat}W
4	1.03×10^{-09}	2.86×10^{-05}
5	9.94×10^{-08}	5.88×10^{-05}
6	4.15×10^{-06}	2.26×10^{-04}
8	6.84×10^{-04}	1.86×10^{-03}
10	1.70×10^{-02}	1.43×10^{-02}
12	0.135	8.85×10^{-02}
14	0.548	0.391
16	1.42	1.20
18	2.82	2.57
20	3.98	4.18
22	5.22	5.92
24	6.52	7.24
26	8.09	8.69
28	9.66	10.3
30	11.7	12.2
35	16.9	17.1
40	23.4	22.8
50	37.2	34.3
60	50.2	46.2
70	61.3	57.1
80	72.0	68.2
90	82.4	79.3
100	92.4	89.5
120	113.	111.
150	144.	144.
200	195.	202.
250	246.	254.
300	296.	306.
350	346.	353.
400	396.	399.
450	446.	446.
500	496.	493.
550	548.	543.
600	598.	593.
650	649.	646.
700	700.	698.
750	751.	762.
800	824.	805.
850	836.	848.
900	870.	891.
950	906.	934.
1000	940.	978.

the escape of third and subsequent pre-compound α-particles is not considered in calculations.

Results obtained using various intranuclear cascade models are shown in Fig. 2. The DISCA-C code gives the reasonable description of experimental data. DISCA-S and CASCADE/INPE better reproduce experimental σ_α^{non} values [44, 46] below 80 MeV.

The total helium isotope production cross-section for proton induced reactions on ^{197}Au calculated by different codes is compared with experimental data in Figs. 3, 4.

Fig. 3 shows measured α-production cross-section [42–44, 46–49], results of calculations by the GNASH and ALICE/ASH codes and the systematics values. The calculations were performed using different models describing the nuclear level density [10, 11, 16, 23, 27]. The good agreement is observed between experimental data and cross-sections calculated by the ALICE/ASH code using the superfluid nuclear model [27] and the Fermi gas model [10] at primary proton energies below 80 MeV. At the energy around 160 MeV the α-particle production cross-section calculated by the Fermi gas model [10] is in a better agreement with experimental data than the cross-sections obtained using the superfluid model. The GNASH code overestimates the α-particle yield comparing with experimental data.

Fig. 4 shows the total α-particle and ^{3}He production cross-section calculated using the DISCA-C code, the DISCA-S code and CASCADE/INPE code. The calculated values are in general agreement with the measured data [32, 42–44, 46–50].

The comparison of model calculations with experimental data shows that the reasonable evaluation of the helium production cross-section can be done using the ALICE/ASH code, the DISCA-C or DISCA-S codes and the CASCADE/INPE code.

4 Evaluation of helium production cross-section

Helium production cross-section has been calculated as a of cross-sections of ^{4}He (σ_α) and ^{3}He ($\sigma_{^3He}$) formation

$$\sigma_{He} = \sigma_\alpha + \sigma_{^3He} \quad (3)$$

The evaluation of the helium isotope production cross-sectior was performed using the results of model calculations, predictions of systematics and available experimental data.

4.1 Proton induced reactions

Fig. 5 shows the α-particle particle production cross-section for ^{181}Ta calculated by different nuclear models, systematics values and measured data [43, 44, 51]. The detail view of the energy range below 200 MeV, which corresponds to the rapid

Table 2. The evaluated helium production cross-section ($\sigma_{\alpha} + \sigma_{^3He}$) for ^{181}Ta and natural tungsten irradiated with neutrons at energies from 5 MeV up to 1 GeV. (Data below 5 MeV can be found in JEFF-3/A.)

Neutron energy (MeV)	Helium production cross-section (mb)	
	^{181}Ta	^{nat}W
5	1.49×10^{-05}	2.88×10^{-03}
6	1.73×10^{-04}	5.41×10^{-03}
7	6.27×10^{-04}	1.15×10^{-02}
8	3.26×10^{-03}	2.54×10^{-02}
9	1.00×10^{-02}	5.88×10^{-02}
10	3.36×10^{-02}	0.132
11	8.00×10^{-02}	0.304
12	0.182	0.609
13	0.335	0.987
14	0.570	1.42
14.5	0.719	1.65
15	0.868	1.88
16	1.23	2.42
17	1.71	2.98
18	2.28	3.49
19	2.91	4.06
20	3.61	4.79
22	5.18	6.03
24	6.94	8.02
26	8.87	10.2
28	11.0	12.5
30	13.1	14.9
35	18.9	21.0
40	25.0	26.3
45	31.1	31.6
50	36.7	35.7
60	47.2	43.5
70	57.2	51.5
80	65.9	60.0
90	72.8	66.2
100	78.5	73.2
120	91.2	86.7
150	112.	109.
200	152.	151
250	200.	194.
300	248.	245.
400	362.	365.
500	480.	477.
600	590.	586.
700	697.	695.
800	801.	807.
900	870.	905.
1000	939.	977.

change in the cross-section value, is given in upper Fig. 5. There is the good agreement between obtained cross-sections and experimental data.

To obtain the cross-sections for natural tungsten the calculations were performed for tungsten isotopes with atomic number A = 180, 182–184 and 186. Fig. 6 shows the α-particle production cross-section calculated by the ALICE/ASH code, the DISCA-S code and the CASCADE/INPE code, systematics values and experimental data [50]. Also the data from ENDF/B-VI and JENDL-HE [52] are shown. There is the good agreement between the cross-sections calculated with the help of the DISCA-S code and the experimental data [50] at 750 MeV. Data from JENDL-HE are in the agreement with systematics values at 62 and 90 MeV and with the cross-sections calculated by the ALICE/ASH code at energies from 100 to 150 MeV.

The results of calculations, systematics values and available measured data were used for the evaluation of the helium production cross-section for ^{181}Ta and natural tungsten. The evaluated data are shown in Fig. 7 and in Table 1.

4.2 Neutron induced reactions

Experimental data for helium isotope production are absent at energies above 15 MeV for ^{181}Ta and for tungsten isotopes. The evaluation was based mainly on the results of calculations. Corrections were made at the energy below 15 MeV using the EXFOR data.

The (n, α) reaction cross-section for tungsten isotopes with A = 180, 182 and 183 was taken from JEFF-3/A at the energies below 20 MeV. New evaluation was performed for the (n, α) reaction cross-section for ^{184}W and ^{186}W using the data from EXFOR. The cross-sections for (n, nα) and (n, ^{3}He) reactions were taken from JEFF-3/A. The data obtained for natural tungsten below 20 MeV were adjusted to the results of calculations at the energies above 20 MeV.

Evaluated helium production cross-sections are shown in Table 2.

5 Conclusion

The comparison of different methods of calculation and computer codes used to obtain helium isotope production cross-section for nuclear reactions induced by nucleons at energies up to 1 GeV has been performed. The result shows that the reasonable evaluation of the helium production cross-section can be done using the ALICE/ASH code, the DISCA code and the CASCADE/INPE code.

The evaluation of the helium isotope production cross-section was performed using the results of model calculations, available experimental data and systematics predictions.

The cross-sections obtained (Table 1, 2) can be used for the evaluation of the helium production rate in tantalum and tungsten irradiated with neutrons and protons at energies up to 1 GeV.

(Received on 13 January 2005)

References

1 *Rubbia, C. et al.*: TRADE (TRIGA Accelerator Driven Experiment): A full Experimental Validation of the ADS concept. Proc. Accelerator Applications in a Nuclear Renaissance (AccApp'03), San Diego, California, June 1–5, 2003

2 *Young, P. G.; Arthur, E. D.; Chadwick, M. B.:* Comprehensive nuclear model calculations: theory and use of the GNASH code. Proc. Int. Atomic Energy Agency Workshop on Nuclear Reaction Data and Nuclear Reactors, April 15–May 17, 1996, Vol. 1, p. 227; LA-12343-MS, Los Alamos National Laboratory Report, Iss. 1992; GNASH-FKK: Pre-equilibrium, Statistical Nuclear-Model Code System for Calculation of Cross Sections and Emission Spectra. RSIC Code Package PSR-125

3 *Williams, F. C.:* Particle-hole state density in the uniform spacing model. Nucl. Phys. A 166 (1971) 231

4 *Kalbach, C.:* Exciton number dependence of the Griffin model two-body matrix element. Z. Phys. A 287 (1978) 319

5 *Kalbach, C.:* The Griffin model, complex particles and direct nuclear reactions. Z. Phys. A 283 (1977) 401

6 *Chadwick, M. B.; Young, P. G.; George, D. C.; Watanabe, Y.:* Multiple preequilibrium emission in Feshbach-Kerman-Koonin analyses. Phys. Rev. C 50 (1994) 996

7 *Konobeyev, A.Yu.; Fukahori, T.; Iwamoto, O.:* Nuclear data evaluation for ^{238}Pu, ^{239}Pu, ^{240}Pu, ^{241}Pu and ^{242}Pu irradiated by neutrons and protons at the energies up to 250 MeV. JAERI-Research 2002–029, Japan Atomic Energy Research Institute Report, Iss. Dec. 2002

8 *Hauser, W.; Feshbach, H.:* The inelastic scattering of neutrons. Phys. Rev. 87 (1952) 366

9 *Chadwick, M. B.; Young, P. G.; Oblozinsky, P.; Marcinkowski, A.:* Preequilibrium spin effects in Feshbach-Kerman-Koonin and exciton models and application to high-spin isomer production. Phys. Rev. C 49 (1994) R 2885

10 *Ignatyuk, A. V.; Smirenkin, G. N.; Tishin, A. S.:* Phenomenological description of the energy dependence of the level density parameter. Sov. J. Nucl. Phys. 21 (1975) 255

11 *Ignatyuk, A. V.:* Level densities. In: Handbook for Calculations of Nuclear Reaction Data. IAEA-TECDOC-1034. International Atomic Energy Agency Report, Iss. 1998, p. 65; http://www-nds.iaea.or.at/ripl/ripl_handbook.htm

12 *Koning, A. J.; Delaroche, J. P.:* Local and global nucleon optical models from 1 keV to 200 MeV. Nucl. Phys. A 713 (2003) 231; data are taken from http://ndswebserver.iaea.org/RIPL-2/

13 *Avrigeanu, V.; Hodgson, P. E.; Avrigeanu, M.:* Global optical potentials for emitted alpha particles. Phys. Rev. C 49 (1994) 2136

14 *Blann, M.; Vonach, H. K.:* Global test of modified precompound decay models. Phys. Rev. C 28 (1983) 1475

15 *Weisskopf, V. F.; Ewing, D. H.:* On the yield of nuclear reactions with heavy elements. Phys. Rev. 57 (1940) 472

16 *Blann, M.:* ALICE-91: Statistical model code system with fission competition. RSIC CODE PACKAGE PSR-146.

17 *Konobeyev, A. Yu.; Korovin, A. Yu.:* Calculation of pre-compound alpha-particle spectra for nucleon induced reactions on the basis of the hybrid exciton model. Kerntechnik 59 (1994) 72

18 *Konobeyev, A. Yu.; Lunev, V. P.; Shubin, Yu. N.:* Pre-equilibrium emission of clusters. Acta Physica Slovaca 45 (1995) 705

19 *Konobeyev, A. Yu.; Korovin, Yu. A.:* Calculation of deuteron spectra for nucleon induced reactions on the basis of the hybrid exciton model taking into account direct processes. Kerntechnik 61 (1996) 45

20 *Konobeyev, A. Yu.; Korovin, Yu. A.; Pereslavtsev, P. E.:* Calculation of fast gamma-emission spectra for reactions induced by intermediate energy particles. Izvestija Vuzov. Ser.: Yadernaja Energetika (Transactions of High School. Ser.: Nuclear Power Engineering) 1 (1997) 2

21 *Konobeyev, A. Yu.; Korovin, Yu. A.; Pereslavtsev, P. E.:* Code ALICE/ASH for calculation of excitation functions, energy and angular distributions of emitted particles in nuclear reactions. Obninsk Institute of Nuclear Power Engineering, Iss. 1997

22 *Dityuk, A. I.; Konobeyev, A. Yu.; Lunev, V. P.; Shubin, Yu. N.:* New advanced version of computer code ALICE-IPPE. INDC (CCP)-410, International Atomic Energy Agency Report, Iss. 1998

23 *Shubin, Yu. N.; Lunev, V. P.; Konobeyev, A. Yu.; Dityuk, A. I.:* Cross-section library MENDL-2 to study activation and transmutation of materials irradiated by nucleons of intermediate energies. INDC (CCP)-385, International Atomic Energy Agency Report, Iss. 1995

24 *Konobeyev, A. Yu.; Korovin, Yu. A.; Vecchi, M.:* Fission product yields in nuclear reactions induced by intermediate energy particles. Kerntechnik 64 (1999) 216

25 *Iwamoto, A.; Harada, K.:* Mechanism of cluster emission in nucleon-induced preequilibrium reactions. Phys. Rev. C 26 (1982) 1821

26 *Sato, K.; Iwamoto, A.; Harada, K.:* Pre-equilibrium emission of light composite particles in the framework of the exciton model. Phys. Rev. C 28 (1983) 1527

27 *Ignatyuk, A. V.; Istekov, K. K.; Smirenkin, G. N.:* Yadernaja Fizika 29 (1979) 875

28 *Konobeyev, A. Yu.; Korovin, Yu. A.; Pereslavtsev, P. E.; Fischer, U.; von Möllendorff, U.:* Development of methods for calculation of deuteron-lithium and neutron-lithium cross-sections for energies up to 50 MeV. Nucl. Sci. Eng. 139 (2001) 1

29 *Konobeyev, A. Yu.; Korovin, Yu. A.:* Application of the intranuclear cascade evaporation model. Kerntechnik 63 (1968) 124

30 *Bunakov, V. E.; Nesterov, M. M.; Tarasov, I. A.:* Applicability of a modified intranuclear-cascade method in nucleon reactions at low and medium energies. Bulletin of the Academy of Sciences of the USSR. Physical Series 41(10) (1977) 168; Izvestiya Akademii Nauk SSSR. Seriya Fizicheskaya 41 (1977) 2187

31 *Chatterjee, A.; Murthy, K. H. N.; Gupta, S. K.:* Optical reaction cross sections for light projectiles. INDC (IND)-27/GJ, International Atomic Energy Agency (1980)

32 *Barashenkov, V. S.; Toneev, V. D.:* Interaction of high energy particles and atomic nuclei with nuclei. Atomizdat, Moscow, 1972

33 *Denisov, F. P.; Mekhedov, V. N.:* Nuclear reactions at high energies. Atomizdat, Moscow, 1972

34 *Konobeyev, A. Yu.; Korovin, Yu. A.:* Helium production cross sections in structural materials irradiated by protons and neutrons at energies up to 800 MeV. J. Nucl. Mater. 195 (1992) 286

35 *Dostrovsky, I.; Fraenkel, Z.; Friedlander, G.:* Monte Carlo calculations of nuclear evaporation processes. III. Applications to Low-Energy Reactions. Phys. Rev. 116 (1959) 683

36 *Barashenkov, V. S.; Kostenko, B. F.; Zadorogny, A. M.:* Time-dependent intranuclear cascade model. Nucl. Phys. A338 (1980) 413

37 *Barashenkov, V. S.:* Monte Carlo simulation of ionization and nuclear processes initiated by hadron and ion beams in media. Computer Physics Communications 126 (2000) 28

38 *Konobeyev, A. Yu.; Fukahori, T.; Iwamoto, O.:* Neutron and proton nuclear data evaluation for ^{235}U and ^{238}U at energies up to 250 MeV. JAERI-Research 2002–028, Japan Atomic Energy Research Institute Report, (Dec. 2002)

39 *Konobeyev, A. Yu.; Lunev, V. P.; Shubin, Yu. N.:* Semi-empirical systematics for (n,α) reaction cross-section at the energy of 14.5 MeV. Nucl. Instr. Meth. B 108 (1996) 233

40 *Konobeyev, A. Yu.; Korovin, Yu. A.:* Use of systematics to estimate neutron reaction cross-sections (systematics at 14.5 and 20 MeV). Atomic Energy 85 (1998) 556

41 *Hendricks, J. S.; Mckinney, G. W.; Waters, L. S.; Roberts, T. L. et al.:* MCNPX extensions. Version 2.5.0. LA-UR-04–0570, Los Alamos National Laboratory (Feb. 2004)

42 *Dubost, H.; Lefort, M.; Peter, J.; Tarrago, X.:* ^{4}He and ^{3}He particles from Au, Bi, and Th nuclides bombarded by 157-MeV protons. Phys. Rev. 136 (1964) B1618

43 *Dubost, H.; Gatty, B.; Lefort, M.; Peter, J.; Tarrago, X.;* Deutons, tritons et hélions d'interaction directe projetés par des protons de 156 MeV a partir de noyaux moyens et lourds. J. de Physique 28 (1967) 257

44 *Muto, J.; Iton, H.; Okano, K.; Shiomi, N.; Fukuda, K.; Omori, Y.; Kinara, M.:* Alpha-particles from several elements bombarded with 30, 43 and 56 MeV protons. Nucl. Phys. 47 (1963) 19

45 *Lefort, M.; Cohen, J. P.; Dubost, H.; Tarrago, X.:* Evidence for nucleon clustering from high-energy reactions. Phys. Rev. 139 (1965) B 1500

46 *Kantelo, M. V.; Hogan, J. J.:* Radiochemical study of alpha particle emission in reactions of ^{202}Hg with 10–86 MeV protons. Phys. Rev. C 13 (1976) 1095

47 *Milazzo-Colli, L.; Braga-Marcazzan, G. M.; Milazzo, M.; Signorini, C.:* Preformation probability of alpha-clusters in rare earth nuclei measured by means of the (p,α) reaction. Nucl. Phys. A 218 (1974) 274

48 *Bertrand, F. E.; Peelle, R. W.:* Complete hydrogen and helium particle spectra from 30- to 60-MeV proton bombardment of nuclei with

A = 12 to 209 and comparison with the intranuclear cascade model. Phys. Rev. C 8 (1973) 1045
49 *Mekhedov, B. N.; Mekhedov, V. N.:* (1970), cited by Ref. [32]
50 *Green, S. L.; Green, W. V.; Hegedus, F. H.; Victoria, M.; Sommer, W. F.; Oliver, B. M.:* Production of helium by medium energy (600 and 800 MeV) protons. J. Nucl. Mater. 155/157 (1988) 1350
51 *Hilscher, D.; Herbach, C.-M.; Jahnke, U.; Tishchenko, V.; Enke, M.; Filges, D.; Goldenbaum, F.; Neef, R.-D.; Nünighoff, K.; Paul, N.; Schaal, H.; Sterzenbach, G.; Letourneau, A.; Böhm, A.; Galin, J.; Lott, B.; Péghaire, A.; Pienkowski, L.:* Helium production for 0.8–2.5 GeV proton induced spallation reactions, damage induced in metallic window materials. J. Nucl. Mater. 296 (2001) 83
52 JENDL high energy data file 2004; http://wwwndc.tokai.jaeri.go.jp/jendl/jendl.html#jendl-sp

The authors of this contribution

C. H. M. Broeders and *A. Yu. Konobeyev**, Institut für Reaktorsicherheit, Forschungszentrum Karlsruhe GmbH, 76021, Karlsruhe, Germany
* Corresponding author. E-mail: konobeev@irs.fzk.de.
Tel. +49 7247 822638

Books · Bücher

Beneficial Uses and Production of Isotopes – 2005 Update. Published by the OECD/NEA 2005. ISBN 92-64-00880-2, 64 pages, 24.00 EUR.

In 2002, isotopes were produced for domestic use and/or international markets in 26 countries (as reported in the survey responses) and more than 30 additional countries were likely producers of isotopes, although they did not respond to the questionnaire. Isotopes were mainly produced in multipurpose research reactors, dedicated isotope production reactors and accelerators. While most research reactors produce isotopes as a by-product to their primary mission, accelerators (except for a few high-energy research machines) are generally dedicated to isotope production. Research reactors are aging with around half of them more than 35 years old. There are, however, at least 11 reactors being built or projected to be built in a number of countries with high-flux reactors being planned for France, Germany, China and Russia. The number of accelerators producing isotopes, especially small dedicated facilities, is growing steadily with the majority of machines being of relatively recent vintage.

Public entities own and operate almost all the research reactors, large-scale accelerators and chemical separation facilities being used for isotope production. Historically, the very large capital requirements, extensive planning and licensing time demands, and additional operating expenses have made public ownership necessary in most cases. Through public-owned facilities, governments offer infrastructure for isotope production and provide for the education and training of the qualified manpower required in the field. These public-owned facilities also often play a critical role of supporting the initial production for research and clinical trials prior to the commercialisation of any pronllsing application. There is, however, a continuing trend toward privatisation and, for example, two privately owned reactors dedicated to isotope production have been built in Canada and are expected to be operational in the near future. A number of medium-sized cyclotrons producing major isotopes for medical applications are owned and operated by private sector enterprises for their exclusive uses as well. Most small cyclotrons, dedicated to the production of medical isotopes, are owned and operated by private enterprises.

Trends in isotope production vary according to the various production facility types and to the geographic region being considered. In particular, trends appear to be different for facilities dedicated to isotope production, such as cyclotrons producing isotopes for medical applications, and for facilities that produce isotopes only as a side activity such as most research reactors. Recent additions to the isotope production capabilities in several regions show a trend to the emergence of private or semi-private producers in response to increasing demand, where this is commercially viable. The security of supply of the major isotopes used in the medical and industrial fields does not appear to be an issue for the short or medium term. However, the ageing infrastructure in a number of important areas such as high-flux research reactors, which are the sole means of production of certain types of isotopes, and the uncertainty for their replacement, leaves questions over the long-term. It is important to ensure a redundancy mechanism in order to secure the supply, in each country, of critical short half-life isotopes such as ^{99}Mo, irrespective of technical (e. g. facility failure), social (e. g. strike) or international (terrorist event closing borders) problems that procurers may encounter.

There are isotope uses in nearly every sector of the economy and in nearly all countries of the world. Isotopes have been used in nuclear medicine since 1946 (^{14}C at the University of Chicago) and routinely for several decades. Nuclear medicine is characterised by an ongoing evolution of techniques arid the continued emergence of new procedures requiring the production of new isotopes or new applications for existing isotopes. Globally, the number of medical procedures involving the use of isotopes is constantly growing and these procedures require an increasing diverse spectrum of isotopes. In industry, isotope uses are very diverse and their relative importance in the various sectors , differs greatly. However, in general, isotopes occupy niche markets where they are more efficient than alternatives or have no substitute. Non-nuclear alternatives are often preferred when they are economically comparable.

The information collected for this study underscores the critical role of governments and public sector entities in isotope production and use. Though the direct responsibilities of governments in the field of isotopes are normally limited to the establishment of safety regulations and the control of compliance with those regulations, national policy, an research and development and medical care, for example, remains a key driver for demand of isotopes and, although to a lesser extent, for their production. However, with the increasing involvement of private companies and the shift to more commercial management of the activities related to isotopes production and uses, governments may want to consider additional support to ensure the stable production of isotopes for research and noncommercial uses within the framework of their national policies, given the importance of beneficial uses of isotopes for science and human welfare.